Journal of the Nigerian Association of Mathematical Physics
Volume32,(November, 2015), **pp 333 – 346**

Mathematical Interactional Analysis of the Dynamics of Livestock Rearing on the Fertile Topsoil

[1]Sarki D.S., [2]Mbah G.C.E and [3]Dikop M.

[1]Department of Mathematics, Federal College of Education Pankshin, Plateau State, Nigeria
[2]Department of Mathematics, University of Nigeria, Nigeria.
[3]Department of Mathematics, Federal College of Education Pankshin, Plateau State, Nigeria.

Abstract

In this paper asystem of deterministic modelispresented and analysed to studythe potentiality of animal rearing on the organic dynamics of vegetation coveron topsoil. We obtained the effective basic depletion ratio,$\mathcal{D}_R$, which was used to determine the conditions for the systems local and global stabilities. Bifurcation analysis was carried out using the centre manifold theory which revealed that the model possesses the forward type. Sensitivity analysis showed that the both human and natural activities as well as environmental advocacy campaigns have very similar but varying decrement impacts on vegetation. It is also shown that a sustainable combination of manure harvest and livestock density can improve soil vegetation. It is further shown that the reallocation of soils to non-agricultural purpose also has negative consequence on vegetation.

1.0 Introduction

Animal production (livestock) is globally considered to be done on a greater percentage of agricultural land [1]. In its report, FAO and others outlined the enormous contribution of animal production (livestock) sector to the global agricultural GDP where it is estimated to employ over a billion people apart from being the major source of livelihoods for a billion people, majority of who represent the world's poor [1]. Livestock products are very rich source protein, other essential micronutrients [2]. These nutrients include minerals such as iron and zinc. However, it is being feared that about 925 million of the world's population are seriously undernourished for lack of appropriate and sufficient food supply[3, 4]. Livestock by-products are the major raw materials for a range of essential household productsand farm manure [2]. In developing countries for instance, draught animals are estimated to provide 80% of the power used for farming [5]. It is estimated that about 52 percent of draught power comes from animals. In India, selling cattle dung for fuel to urban centres can supply up to 60% of the income of the poor village family. Its prospects in developing countries are bright following its increasing dietary preference over staple food. The number of ruminant animals (like goats and sheep) produced per unit of agricultural area in developing countries is almost double that of undeveloped countries. However, eminent challenges of this on scarce resources such as arable land and water are serious concerns [6]. A high livestock density has implications on soil nutrients and other organic matter content utilization and environmental pollution in addition to the attendant health implication from habitually consumptionof a livestock-dominant dietary composition. Furthermore, animal agriculture contributes to greenhouse gas emission in the form of carbondioxide, methane and nitrous oxide [7, 8] with Africa feared to be worst hit [6]. From the foregoing, an understanding of the ecological and other aspects of animal agriculture is critical to ensure access to safe and healthy food and sustainable environment [9, 10]. Factors influencing animal production and utilisation range from mechanical like farm management and soil condition among others [11, 12, 13, 14]; to biological, which include health, temperature, reproduction and nutrition etc.[15, 16, 17, 18]; and management and socio-economic factors [19,20, 21]. There is need to simultaneously consider these factors if efficient management systems of animal traction are to be developed [22].

Corresponding author: Sarki D.S., E-mail: dinsarki@gmail.com, Tel.: +2348069739912, 8034198454(M.G.C.E)

2.0 Model Formulation and Basic Dynamics of Infertility and Cultivation

The total land mass at time *t,* denoted by $\mathcal{S}(t)$, is classified intotwo distinct but relatively interrelated soil masses, vegetated topsoil, $\mathcal{S}_{\mathrm{V}}(t)$ and the non-vegetated bare land mass, $\mathcal{S}_{\mathrm{Nv}}(t)$,so that $\mathcal{S}(t) = \mathcal{S}_{\mathrm{V}}(t) + \mathcal{S}_{\mathrm{Nv}}(t)$.Animal (cattle, small ruminants and birds) population and their interaction (covering activities like grazing, pecking and burrowing) with vegetated topsoilare modelled by the parameters Φ and η_{R}respectively. They are reduced by removals (consumption and mortality) at aremoval rate, ψ.Soil vegetative cover is assumed to increase at a constant rate Δ, the fractions, λ and ξrespectively monitor human-induced vegetation removals (HIVR) and naturally-induced vegetation removal (NIVR), further, non-agriculture land utilisation (NALU),γ, models (in both classes) soil removals due to developmental (construction) purposes. On the other hand non-vegetated bare land is both increased through a constant recruitment rate Γ and vegetation loses of $\mathcal{S}_{\mathrm{V}}(t)$ and then reduced at the rate γ. The assumed removals followed extreme deployable activities on vegetated topsoil. We assume that the stock of manure is accrued either at a constant rate Ωor through animal droppings at a rate $\lambda_{\mathrm{R}}$and reduced by application on farmlands at a rate η_{B}. The deleterious animal-effective-contact rate (AECR), η_{P}, given by

$$\boldsymbol{\eta_{\mathrm{P}}} = \frac{(\boldsymbol{\beta_{\mathrm{A}}} + \boldsymbol{\beta_{\mathrm{E}}})\boldsymbol{\mathcal{S}_{\mathrm{V}}} + \boldsymbol{\phi_{\mathrm{P}}}\boldsymbol{\beta_{\mathrm{E}}}\boldsymbol{\mathcal{S}_{\mathrm{Nv}}}}{\boldsymbol{\mathcal{S}}}$$

where β_{A} and β_{E} are, respectively, the excessive animaland natural effective activity contact rates on$\boldsymbol{\mathcal{S}_{\mathrm{V}}}$ and $\boldsymbol{\mathcal{S}_{\mathrm{Nv}}}$, sufficient for soil degradation (it is assumed that the severity of this rates increases in the order of their arrangement; thus β_{A} is milder while β_{E} is severest); so that as compared with the relative losses on $\boldsymbol{\mathcal{S}_{\mathrm{V}}}$, the modifying parameter, $\boldsymbol{\phi_{\mathrm{P}}}$, models increased degradation index on $\boldsymbol{\mathcal{S}_{\mathrm{Nv}}}$. The formulation of the present model mimics the flow pattern of epidemiological processes and adopted insights from [23,24].

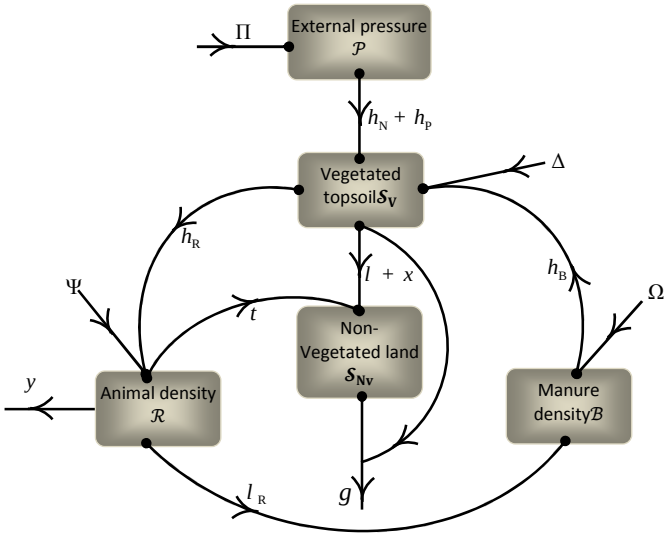

Fig. 1. Model's flow diagram for soil dynamics

2.1 Derivation of Model Equations:

Combining all the aforementioned assumptions and definitions, the model for the dynamics of rearing on a vegetated topsoil is given by the following system of nonlinear differential equations:

$$\begin{aligned}
\frac{d\mathcal{P}}{dt} &= \Pi - (\eta_{\mathrm{P}} + \eta_{\mathrm{N}})\mathcal{P} \\
\frac{d\mathcal{B}}{dt} &= \Omega + \lambda_{\mathrm{R}}\mathcal{R} - \eta_{\mathrm{B}}\mathcal{B} \\
\frac{d\mathcal{R}}{dt} &= \Phi - \psi\mathcal{R} \qquad (1) \\
\frac{d\mathcal{S}_{\mathrm{V}}}{dt} &= \Delta + (\eta_{\mathrm{P}} + \eta_{\mathrm{N}})\mathcal{P} + (\eta_{\mathrm{B}}\mathcal{B} + \eta_{\mathrm{R}}\mathcal{R} - K_1)\mathcal{S}_{\mathrm{V}} \\
\frac{d\mathcal{S}_{\mathrm{Nv}}}{dt} &= \Gamma + \eta_{\mathrm{R}}\mathcal{R}\mathcal{S}_{\mathrm{Nv}} + (\lambda + \xi)\mathcal{S}_{\mathrm{V}} - \gamma\mathcal{S}_{\mathrm{Nv}}
\end{aligned}$$

where$K_1 = \gamma + \lambda + \xi$.

Table 1: Description of model variables

Variable	Description
$\mathcal{P}(t)$	External pressure (both human and natural activities)
$\mathcal{B}(t)$	Aggregate manure
$\mathcal{R}(t)$	Animal population
$\mathcal{S}(t)$	Total land mass
$\mathcal{S}_{\mathrm{V}}(t)$	Mass of vegetated topsoil
$\mathcal{S}_{\mathrm{Nv}}(t)$	Mass of non – vegetated land

The densities described by the system(1)are fundamentally nonnegative, thus all variables and parameter values should be nonnegative [24].Thus to verify that the region, Ω, given by

$\Omega = \{(\mathcal{P}, \mathcal{B}, \mathcal{R}, \mathcal{S}_{\mathrm{V}}, \mathcal{S}_{\mathrm{Nv}}) \in \mathbb{R}^5_+ | \mathcal{S} \leq \Delta/K_1, \mathcal{R} \leq \Phi/\psi\}$,

is a positively attracting one for the system (1), we proceed as follows, noting beforehand that the ensuing dynamics of seed and fertile soil densities are

$$\frac{d\mathcal{S}_{\mathrm{A}}}{dt} = \Delta + (\eta_{\mathrm{N}} + \eta_{\mathrm{P}})\mathcal{P} - K_1\mathcal{S}_{\mathrm{A}}$$

and

$$\frac{d\mathcal{R}}{dt} = \Phi - \psi\mathcal{R}$$

respectively. We note that these densities are particularly maximal whenever $\mathcal{S}_{\mathrm{A}} > \Delta/K_1$and $\mathcal{R} > \Phi/\psi$respectively, with the two derivable whenever$d\mathcal{S}_{\mathrm{A}}/dt < 0$and $d\mathcal{R}/dt < 0$.Since the two rates$d\mathcal{S}_{\mathrm{A}}/dt$and $d\mathcal{R}/dt$ are respectively bounded by $\Delta - K_1\mathcal{S}_{\mathrm{A}}$and $\Phi - \psi\mathcal{R}$ applying the standard comparison theorem ofLakshimikantham and Martynyukas used in [24]it can be shown that these solutions hold:

$$\mathcal{S}_{\mathrm{A}}(t) \leq \mathcal{S}_{\mathrm{A}}(0)e^{-K_1 t} + \Delta/K_1(1 - e^{-K_1 t})$$

and

$$\mathcal{R}(t) \leq \mathcal{R}(0)e^{-\psi t} + \Phi/\psi\left(1 - e^{-\psi t}\right).$$

In the same vain, if

$$\mathcal{S}_{\mathrm{A}}(0) \leq \Delta/K_1$$

and

$$\mathcal{R}(0) \leq \Phi/\psi$$

then

$$\mathcal{S}_{\mathrm{A}}(t) \leq \Delta/K_1$$

and

$$\mathcal{R}(t) \leq \Phi/\psi,$$

respectively. Thus each solution of **Error! Reference source not found.**, with initial conditions in Ω, will remain there for all $t > 0$. Thus confirming the positive-invariance and attracting status of Ω. In consequence, therefore, the dynamics of soil infertility could be considered there,since in this region the model (1)can be considered as being agronomically and mathematically well-posed [25].

2.2 Local stability of rearing-free equilibrium (RFE)

The system (1) has an RFE, $\mathcal{E}_{\mathrm{R}}$, contained in the boundary of $\mathbb{R}^5_+$[26] which is gotten by setting the right hand sides of its equations to zero and given by

$$\boldsymbol{\mathcal{E}^0_{\mathrm{R}}} = (\boldsymbol{\mathcal{P}^*},\ \boldsymbol{\mathcal{B}^*},\ \boldsymbol{\mathcal{R}^*},\ \boldsymbol{\mathcal{S}^*_{\mathrm{V}}},\ \boldsymbol{\mathcal{S}^*_{\mathrm{Nv}}}) = (\mathbf{0}, \mathbf{0}, \boldsymbol{\Phi/\psi}, \boldsymbol{\Delta/K_1}, \mathbf{0}), \quad (2)$$

The subsystem (1)has an RFE, $\boldsymbol{\mathcal{E}^0_{\mathrm{R}}}$contained in the boundary of $\mathbb{R}^5_+$[26] obtained by setting the right hand sides of its equations to zero, and given by

$$\boldsymbol{\mathcal{E}^0_{\mathrm{R}}} = \left(\boldsymbol{\mathcal{P}^0},\ \boldsymbol{\mathcal{B}^0},\ \mathcal{R}^0,\ \boldsymbol{\mathcal{S}^0_{\mathrm{V}}},\ \boldsymbol{\mathcal{S}^0_{\mathrm{Nv}}}\right) = (\boldsymbol{\mathcal{P}^*},\ \boldsymbol{\mathcal{B}^*},\ \mathcal{R}^*,\ \boldsymbol{\mathcal{S}^*_{\mathrm{V}}},\ \boldsymbol{\mathcal{S}^*_{\mathrm{Nv}}}), \quad (3)$$

The linear stability of $\boldsymbol{\mathcal{E}^0_{\mathrm{R}}}$, can be established using the next generation operator method on the system (3), so that the matrices $\mathcal{F}$and $\mathcal{V}$, respectively representing the agronomic terms and all degradative terms, are, respectively given in [27,28]. To simplify our calculation, we evaluate the RFE around the equilibrium $x_0 = (\boldsymbol{\mathcal{P}^*},\ \boldsymbol{\mathcal{B}^*},\ \mathcal{R}^*,\ \boldsymbol{\mathcal{S}^*_{\mathrm{V}}},\ \boldsymbol{\mathcal{S}^*_{\mathrm{Nv}}})$, to get the matrices

$$\boldsymbol{\mathcal{F}} = \begin{pmatrix} \mathbf{0} & \mathbf{0} & \mathbf{0} & \mathbf{0} & \mathbf{0} \\ \mathbf{0} & \mathbf{0} & \mathbf{0} & \mathbf{0} & \mathbf{0} \\ \mathbf{0} & \mathbf{0} & \mathbf{0} & \mathbf{0} & \mathbf{0} \\ \mathbf{0} & \boldsymbol{\eta_{\mathrm{B}}} & \boldsymbol{\eta_{\mathrm{R}}} & \boldsymbol{\beta_{\mathrm{A}} + \beta_{\mathrm{E}}} & \boldsymbol{\phi_{\mathrm{P}}\beta_{\mathrm{E}}} \\ \mathbf{0} & \mathbf{0} & \boldsymbol{\eta_{\mathrm{R}}} & \mathbf{0} & \mathbf{0} \end{pmatrix},$$

And

$$\boldsymbol{\mathcal{V}} = \begin{pmatrix} \boldsymbol{\eta_N} & \mathbf{0} & \mathbf{0} & \mathbf{0} & \mathbf{0} \\ \mathbf{0} & \boldsymbol{\eta_B} & \boldsymbol{-\lambda_R} & \mathbf{0} & \mathbf{0} \\ \mathbf{0} & \mathbf{0} & \boldsymbol{\psi} & \mathbf{0} & \mathbf{0} \\ \boldsymbol{-\eta_N} & \mathbf{0} & \mathbf{0} & \boldsymbol{K_1} & \mathbf{0} \\ \mathbf{0} & \mathbf{0} & \mathbf{0} & \boldsymbol{-(\lambda+\xi)} & \boldsymbol{\gamma} \end{pmatrix}.$$

Thus

$$\mathcal{V}^{-1} = \begin{pmatrix} -\eta_N^{-1} & 0 & 0 & 0 & 0 \\ 0 & -\eta_B^{-1} & \lambda_R/\psi\eta_B & 0 & 0 \\ 0 & 0 & \boldsymbol{\psi^{-1}} & 0 & 0 \\ K_1^{-1} & \mathbf{0} & 0 & K_1^{-1} & 0 \\ (\lambda+\xi)/\gamma K_1 & 0 & 0 & (\lambda+\xi)/\gamma K_1 & \boldsymbol{\lambda^{-1}} \end{pmatrix}$$

The next generation matrix, $\mathcal{G} = \mathcal{F} \times \mathcal{V}^{-1}$, thus becomes

$$\mathcal{G} = \begin{pmatrix} 0 & 0 & 0 & 0 & 0 \\ 0 & 0 & 0 & 0 & 0 \\ 0 & 0 & 0 & 0 & 0 \\ \dfrac{\beta_A+\beta_E}{K_1} + \dfrac{\phi_P\beta_E(\lambda+\xi)}{\gamma K_1} & 1 & \dfrac{\eta_R+\lambda_R}{\psi} & \dfrac{\beta_A+\beta_E}{K_1} + \dfrac{\phi_P\beta_E(\lambda+\xi)}{\gamma K_1} & \dfrac{\phi_P\beta_E}{\gamma} \\ 0 & 0 & \eta_R/\psi & 0 & \mathbf{0} \end{pmatrix}$$

Therefore the spectral radius of the next generation matrix, [27, 28, 29], (respectively with respect to degradation) is

$$\boldsymbol{\mathcal{D}_R} = \frac{\boldsymbol{\gamma\beta_A + \beta_E[\gamma + \phi_P(\lambda+\xi)]}}{\boldsymbol{\gamma K_1}} \qquad (\mathbf{4})$$

The following result follows from Theorem 2 of [27]

Lemma 1: *The RFE of rearing on vegetatedtopsoil model*(1), *given by*(3), *is locally asymptotically stable (LAS) if* $\boldsymbol{\mathcal{D}_R} < 1$ *and unstable if* $\boldsymbol{\mathcal{D}_R} > 1$.

The threshold quantity $\boldsymbol{\mathcal{D}_R}$ as the soil depletion number measures the average of mass of new soil degradation, on a vegetativetopsoil land mass, by a typical causative agent [29].

1.1. Analysis of $\boldsymbol{\mathcal{D}_R}$. The computed threshold quantityis used to determine whether or not rearingona vegetated topsoil can lead to effective degradation management and consequently improve livestock production. Since all model parameters are positive, it is obvious from (4) that

Theorem 2: *The rearing free equilibrium (RFE) is locally asymptotically stable if* $\boldsymbol{\mathcal{D}_R} < 1$.

Proof: We use the Jacobian stability technique to achieve this claim.

The Jacobian of the system (1) around $\boldsymbol{\mathcal{E}_R^0}$ is

$$\boldsymbol{\mathcal{J}(\mathcal{E}_R^0)} = \begin{pmatrix} \boldsymbol{-\eta_N} & \mathbf{0} & \mathbf{0} & \mathbf{0} & \mathbf{0} \\ \mathbf{0} & \boldsymbol{-\eta_B} & \boldsymbol{\lambda_R} & \mathbf{0} & \mathbf{0} \\ \mathbf{0} & \mathbf{0} & \boldsymbol{-\eta_R} & \mathbf{0} & \mathbf{0} \\ \boldsymbol{\eta_N} & \boldsymbol{\eta_B} & \boldsymbol{\eta_R} & \boldsymbol{\beta_A+\beta_E-K_1} & \boldsymbol{\phi_P\beta_E} \\ \mathbf{0} & \mathbf{0} & \boldsymbol{\eta_R} & \boldsymbol{\lambda+\xi} & \boldsymbol{-\gamma} \end{pmatrix} \qquad (\mathbf{5})$$

The row transformed matrix $\boldsymbol{\mathcal{J}(\mathcal{E}_R^0)}$ is as given below

$$\boldsymbol{\mathcal{J}(\mathcal{E}_R^0)} = \begin{pmatrix} \boldsymbol{-\eta_N} & \mathbf{0} & \mathbf{0} & \mathbf{0} & \mathbf{0} \\ \mathbf{0} & \boldsymbol{-\eta_B} & \boldsymbol{\lambda_R} & \mathbf{0} & \mathbf{0} \\ \mathbf{0} & \mathbf{0} & \boldsymbol{-\eta_R} & \mathbf{0} & \mathbf{0} \\ \mathbf{0} & \mathbf{0} & \mathbf{0} & \boldsymbol{\beta_A+\beta_E-K_1} & \boldsymbol{\phi_P\beta_E} \\ \mathbf{0} & \mathbf{0} & \mathbf{0} & \mathbf{0} & \boldsymbol{a} \end{pmatrix} \qquad (\mathbf{6})$$

where

$$a = -\frac{\gamma K_1 - [\gamma(\beta_A+\beta_E) + \phi_P\beta_E(\lambda+\xi)]}{K_1 - (\beta_A+\beta_E)}$$

Thus the corresponding eigenvalues are:

$$\lambda_1 = -\eta_B, \lambda_2 = -\eta_R, \lambda_3 = -\eta_N, \lambda_4 = \beta_A+\beta_E-K_1,$$

$$\lambda_5 = -\frac{\gamma K_1 - [\gamma(\beta_A+\beta_E) + \phi_P\beta_E(\lambda+\xi)]}{K_1 - (\beta_A+\beta_E)}$$

Thus $\lambda_4 < 0$ if $K_1 > (\beta_A+\beta_E)$ and $\lambda_5 < 0$ if $\gamma K_1 > \gamma(\beta_A+\beta_E) + \phi_P\beta_E(\lambda+\xi)$,provided

$$\frac{\gamma(\beta_A+\beta_E) + \phi_P\beta_E(\lambda+\xi)}{\gamma K_1} < 1$$

The result follows immediately from (4).

2.3 Global stability of RFE

Following the procedure in [30] we establish the global stability of the system (1) as follows: firstly, for emphasis, we reproduce the stability scheme of [30], which can also be looked up in [31].

Theorem 3:*Consider a model system that is described by the following differential equations* [30]

$$\frac{d\boldsymbol{X_1}}{dt} = \boldsymbol{\mathcal{F}}(\boldsymbol{X_1}, \boldsymbol{X_2}) \tag{7}$$

and

$$\frac{d\boldsymbol{X_2}}{dt} = \boldsymbol{\mathcal{G}}(\boldsymbol{X_1}, \boldsymbol{X_2}); \boldsymbol{\mathcal{G}}(\boldsymbol{X_1}, \boldsymbol{0}) = \boldsymbol{0}, \tag{8}$$

where $\mathcal{X}_1 \in \mathbb{R}^m$,$\mathcal{X}_2 \in \mathbb{R}^n$ and $\mathcal{X}_0 = (\mathcal{X}_1^*, 0)$denote, respectively, the uninfected, infected components of a given populations and the disease- (in this present sense challenged or compromised, that is, infertility) free equilibrium of the system. Assume further that

(H1). For $\frac{d\mathcal{X}_1}{dt} = \mathcal{F}(\mathcal{X}_1, \mathcal{X}_2)$, $\mathcal{X}_1^*$ is globally asymptotically stable and

(H2). $\mathcal{G}(\mathcal{X}_1, \mathcal{X}_2) = \mathcal{A}\mathcal{X}_2 - \hat{\mathcal{G}}(\mathcal{X}_1, \mathcal{X}_2)$, $\hat{\mathcal{G}}(\mathcal{X}_1, \mathcal{X}_2) \geq 0$for $(\mathcal{X}_1, \mathcal{X}_2) \in \Omega$, where the Jacobian $\frac{d\mathcal{G}}{d\mathcal{X}_1} = \mathcal{F}(\mathcal{X}_1^*, 0)$ is an M-matrix (the off diagonal elements of $\mathcal{A}$ are nonnegative) and Ω is the region where the model makes biological (agronomical) sense.

Then the RFE$\mathcal{X}_0 = (\mathcal{X}_1^*, 0)$ is globally asymptotically stable provided $\mathcal{D}_{\mathrm{R}} < 1$.

From the forgoing we argue as follows:

Theorem 4:*The RFE of the model* (1) is globally asymptotically stable (GAS) in Ω provided $\mathcal{D}_{\mathrm{R}} < 1$

Proof: Conditions (H1) and (H2), of Theorem 1 above needed to be satisfied for $\mathcal{D}_{\mathrm{R}} < 1$. To achieve this, we deduce from(1)that $\mathcal{X}_1 = (\mathcal{P}, \mathcal{S}_{\mathrm{Nv}}) \in \mathbb{R}^2$ and $\mathcal{X}_2 = (\mathcal{B}, \mathcal{C}, \mathcal{S}_{\mathrm{V}}) \in \mathbb{R}^3$ denote our infertility-free and infertile densities respectively. The RFE is$\mathcal{E}_{\mathrm{R}}^0 = (\mathcal{X}_1^0, 0)$, where$\mathcal{X}_1^0 = (\Pi/\eta_{\mathrm{N}}, \Gamma/\gamma)$.

Thus by (H1)together with **Error! Reference source not found.** it will become clear that

$$\frac{d\boldsymbol{X_1}}{dt} = \boldsymbol{\mathcal{F}}(\boldsymbol{X_1}, \boldsymbol{0}) = \begin{pmatrix} \boldsymbol{\Pi - \eta_{\mathrm{N}} \mathcal{P}^0} \\ \boldsymbol{\Omega - \eta_{\mathrm{B}} \mathcal{B}^0} \end{pmatrix} \tag{9}$$

Hence

$$\boldsymbol{\mathcal{P}^0(t)} = \frac{\boldsymbol{\Pi}}{\boldsymbol{\eta_{\mathrm{N}}}} - \frac{\boldsymbol{\Pi}}{\boldsymbol{\eta_{\mathrm{N}}}} \boldsymbol{e^{-\eta_{\mathrm{N}} t}} + \boldsymbol{\mathcal{P}^0(0)} \frac{\boldsymbol{\Pi}}{\boldsymbol{\eta_{\mathrm{N}}}} \boldsymbol{e^{-\eta_{\mathrm{N}} t}} \tag{10}$$

and

$$\boldsymbol{\mathcal{S}_{\mathrm{Nv}}^0(t)} = \frac{\boldsymbol{\Gamma}}{\boldsymbol{\gamma}} - \frac{\boldsymbol{\Gamma}}{\boldsymbol{\gamma}} \boldsymbol{e^{-\gamma t}} + \boldsymbol{\mathcal{S}_{\mathrm{Nv}}^0(0)} \frac{\boldsymbol{\Gamma}}{\boldsymbol{\gamma}} \boldsymbol{e^{-\gamma t}}, \tag{11}$$

Therefore, the mass of soil, when infertility is assumed to be nonexistence is$\mathcal{S}_{\mathrm{Nv}}^0 \longrightarrow \mathcal{S}^0(0)$ as t ® ¥ **,** irrespective of the values of $\mathcal{P}^0(0)$. Hence $\mathcal{X}_1^0$ is globally asymptomatically stable.

Secondly, for $\mathcal{G}(\mathcal{X}_1, \mathcal{X}_2) = \mathcal{A}\mathcal{X}_2 - \hat{\mathcal{G}}(\mathcal{X}_1, \mathcal{X}_2)$, then we will have that

$$\boldsymbol{\mathcal{A}} = \begin{pmatrix} \boldsymbol{-\eta_{\mathrm{B}}} & \boldsymbol{\lambda_{\mathrm{R}}} & \boldsymbol{0} \\ \boldsymbol{0} & \boldsymbol{-\psi} & \boldsymbol{0} \\ \boldsymbol{\eta_{\mathrm{B}}} & \boldsymbol{\eta_{\mathrm{R}}} & \boldsymbol{-K_1} \end{pmatrix} \tag{12}$$

Since all the off-diagonal elements of (12) are nonnegative, then A must be an M-matrix.

$$\mathcal{G}(\mathcal{X}_1, \mathcal{X}_2) = \begin{pmatrix} \Omega + \lambda_{\mathrm{R}}\mathcal{R} - \eta_{\mathrm{B}}\mathcal{B} \\ \Phi - \psi\mathcal{R} \\ \Delta + [\eta_{\mathrm{B}}\mathcal{B} + \eta_{\mathrm{R}}\mathcal{R} - K_1]\mathcal{S}_{\mathrm{V}} \end{pmatrix} \tag{13}$$

therefore$\hat{\mathcal{G}}(\mathcal{X}_1, \mathcal{X}_2) = \mathcal{A}\mathcal{X}_2 - \mathcal{G}(\mathcal{X}_1, \mathcal{X}_2) = 0$, since obviously

$$\boldsymbol{\widehat{\mathcal{G}}(\mathcal{X}_1, \mathcal{X}_2)} = (\boldsymbol{0}, \boldsymbol{0})^{\boldsymbol{T}}. \tag{14}$$

Note: this follows from the expression for $\boldsymbol{\mathcal{X}_2}$as well as the (12) and (13).The proofthus follows.

2.4 Existence of the continuesrearing free (endemic) equilibrium state $\mathcal{E}^*$

The conditions for the continues non livestock rearing on vegetated topsoil (the case where not all of $\mathcal{P}, \mathcal{B}, \mathcal{R}, \mathcal{S}_{\mathrm{V}}, \mathcal{S}_{\mathrm{Nv}}$), denoted by $\boldsymbol{\mathcal{E}_{\mathrm{R}}^*} = (\boldsymbol{\mathcal{P}^*}, \boldsymbol{\mathcal{B}^*}, \mathcal{R}^*, \boldsymbol{\mathcal{S}_{\mathrm{V}}^*}, \boldsymbol{\mathcal{S}_{\mathrm{Nv}}^*})$, have zero density, a situation derivable when the coordinates of the equations in (1) satisfy the conditions described below:

$$\boldsymbol{\mathcal{E}_{\mathrm{R}}^*} = \{(\boldsymbol{\mathcal{P}^*}, \boldsymbol{\mathcal{B}^*}, \boldsymbol{\mathcal{R}^*}, \boldsymbol{\mathcal{S}_{\mathrm{V}}^*}, \boldsymbol{\mathcal{S}_{\mathrm{Nv}}^*}) | \boldsymbol{\mathcal{P}^*} > 0, \boldsymbol{\mathcal{B}^*} > 0, \boldsymbol{\mathcal{R}^*} > 0, \boldsymbol{\mathcal{S}_{\mathrm{V}}^*} > 0, \boldsymbol{\mathcal{S}_{\mathrm{Nv}}^*} > 0\} \tag{15}$$

Lemma 5:*The continues non-rearingon vegetated topsoil equilibrium of the model* (1) *exists whenever the effective depletion ratio,* $\mathcal{D}_{\mathrm{R}}$*is greater than unity*

Proof: At the persistence equilibrium state, let

$$(\boldsymbol{\mathcal{P}}, \boldsymbol{\mathcal{B}}, \boldsymbol{\mathcal{R}}, \boldsymbol{\mathcal{S}_{\mathrm{V}}}, \boldsymbol{\mathcal{S}_{\mathrm{Nv}}}) = (\boldsymbol{\mathcal{P}^*}, \boldsymbol{\mathcal{B}^*}, \boldsymbol{\mathcal{R}^*}, \boldsymbol{\mathcal{S}_{\mathrm{V}}^*}, \boldsymbol{\mathcal{S}_{\mathrm{Nv}}^*}) \tag{16}$$

However we note that the expression for $\mathcal{D}_R$ (see (4)) isindependent of both manure livestock densities, thus suppressing all traces of the two in the remaining four compartments of(1)gives the following

$$\boldsymbol{\mathcal{P}^* = \frac{\Pi}{\eta_P^* + \eta_N^*}, \mathcal{S}_V^* = \frac{\Delta + \Pi}{K_1}, \mathcal{S}_{Nv}^* = \frac{K_1\Gamma + (\lambda + \xi)(\Delta + \Pi)}{\gamma K_1}} \quad (17)$$

Substituting (17) in the expression for η_P^*we observe the following:

$$\mathcal{S}^* = \mathcal{S}_V^* + \mathcal{S}_{Nv}^* = \frac{K_1\Gamma + (\gamma + \lambda + \xi)(\Delta + \Pi)}{\gamma K_1},$$

Thus

$$\eta_P^* = \frac{\phi_P\beta_E K_1\Gamma + [\gamma(\beta_A + \beta_E) + \phi_P\beta_E(\lambda + \xi)](\Delta + \Pi)}{K_1(\Gamma + \Delta + \Pi)}$$

or

$$\boldsymbol{\eta_P^* K_1(\Gamma + \Delta + \Pi) - \phi_P\beta_E K_1\Gamma - [\gamma(\beta_A + \beta_E) + \phi_P\beta_E(\lambda + \xi)](\Delta + \Pi) < 0} \quad (18)$$

It can easily be for verified that $\phi_P\beta_E K_1\Gamma + [\gamma(\beta_A + \beta_E) + \phi_P\beta_E(\lambda + \xi)](\Delta + \Pi) < \gamma K_1$

whichcan easily be simplified to give

$$\frac{[\gamma(\beta_A + \beta_E) + \phi_P\beta_E(\lambda + \xi)](\Delta + \Pi)}{\gamma K_1} < 1 \text{ or} \mathcal{D}_R > 1$$

as required.

Hence the system(1) has a unique positive solution of the form

$$\eta_P^* = \frac{\phi_P\beta_E K_1\Gamma + [\gamma(\beta_A + \beta_E) + \phi_P\beta_E(\lambda + \xi)](\Delta + \Pi)}{K_1(\Gamma + \Delta + \Pi)}$$

provided $\mathcal{D}_R > 1$.Thus we conclude as follows

Lemma 6. *The system* (1)*has a unique persistence equilibrium whenever* $\mathcal{D}_R > 1$ *and none when otherwise*

2.5 Local stability of Persistence Equilibrium

The computational involvement of the procedure for the standard linearization, about the equilibrium, of a system is quite cumbersome and barely mathematically tractable thus making the method unfavourable. We use the manifold theory, described in [32] and reproduced here as Theorem 7, which is evidently most preferred [24]), to establish the local asymptotic stability of the persistence equilibrium.

Theorem 7. Bifurcation Theorem [32]

Consider the general system of ordinary differential equations with parameter ϕ

$$\boldsymbol{\frac{dx}{dt} = f(x, \phi), f: \mathbb{R}^n \times \mathbb{R} \longrightarrow \mathbb{R} \text{ and } f \in \mathbb{C}^2(\mathbb{R}^n \times \mathbb{R}),} \quad (19)$$

where 0 is an equilibrium point of the system, that is $\boldsymbol{f(0, \phi) \equiv 0\ \forall \phi}$,and assume that:

1. $\mathcal{A} = \mathcal{D}_x f(0,0) = \left(\frac{\partial f_i}{\partial x_j}(0,0)\right)$ is the linearization matrix of the system (19)around the equilibrium 0 with f evaluated at zero. Zero is a simple eigenvalue of A and other eigenvalues of A have negative real parts;
2. A has a right and left eigenvectors, W and V, respectively; each corresponding to the zero eigenvalue.

Let f_k be the k^{th} component of *f* and

$$\boldsymbol{a = \frac{1}{2}\sum_{k,i,j=1}^{n} v_k w_i w_j \frac{\partial^2 f_k}{\partial x_i \partial x_j}(0,0) \text{ and } b = \sum_{k,i=1}^{n} v_k w_i \frac{\partial^2 f_k}{\partial x_i \partial \phi}(0,0)} \quad (20)$$

Then the local dynamics of the system (19) around the equilibrium point 0 is totally determined by the signs of a and b.

i. $a > 0, b > 0$. When $\phi < 0$with $|\phi| \ll 1$,0 is locally asymptotically stable and there exists a positive unstable equilibrium; when $0 < \phi \ll 1$, 0 is unstable and there exists a negative locally asymptomatically stable equilibrium;
ii. $a < 0, b < 0$. When $\phi < 0$ with $|\phi| \ll 1$,0 is unstable; when $0 < \phi \ll 1$, 0 is a locally asymptotically stable equilibrium, and there exists a positive unstable equilibrium;
iii. $a > 0, b < 0$. When $\phi < 0$with $|\phi| \ll 1$, 0 is unstable, and there exists a locally asymptotically stable negative equilibrium; when $0 < \phi \ll 1$, 0 is stable and there exists a positive un stable equilibrium;
iv. $a < 0, b > 0$. When ϕ changes from negative to positive, 0 changes its stability from stable to unstable. Correspondingly, a negative unstable equilibrium becomes positive and locally asymptomatically stable.

Note: if $a > 0$and$b > 0$ then a backward bifurcation occurs at $\phi = 0$.
To organise our ensuing system for computational convenience, consider the following simplifications and change of variables: let

$$\mathcal{P} = x_1, \mathcal{B} = x_2, \mathcal{C} = x_3, \mathcal{S}_{\mathrm{V}} = x_4 \text{and } \mathcal{S}_{\mathrm{Nv}} = x_5 \Longrightarrow \mathcal{S} = \mathcal{S}_{\mathrm{V}} + \mathcal{S}_{\mathrm{Nv}} = x_4 + x_5;$$

further, using the vector notation

$$X = (x_1, x_2, x_3, x_4, x_5)^t$$

the subsystem (1) takes the form

$$\frac{dX}{dt} = (f_1, f_2, f_3, f_4, f_5)^t$$

and described as follows:

$$\begin{aligned}
\frac{dx_1}{dt} &= f_1 = \Pi - (\eta_{\mathrm{P}} + \eta_{\mathrm{N}})x_1 \\
\frac{dx_2}{dt} &= f_2 = \Omega + \lambda_{\mathrm{R}} x_3 - \eta_{\mathrm{B}} x_2 \\
\frac{dx_3}{dt} &= f_3 = \Phi - \psi x_3 \\
\frac{dx_4}{dt} &= f_4 = \Delta + (\eta_{\mathrm{P}} + \eta_{\mathrm{N}})x_1 + (\eta_{\mathrm{B}} x_2 + \eta_{\mathrm{R}} x_3 - K_1)x_4 \\
\frac{dx_5}{dt} &= f_5 = \Gamma + \eta_{\mathrm{R}} x_3 x_5 + (\lambda + \xi)x_4 - \gamma x_5
\end{aligned} \tag{21}$$

Considering γ^* as a bifurcation parameter, then its expression from (4) presently becomes

$$g^* = \frac{f_{\mathrm{p}} b_{\mathrm{E}} (l + x)}{K_1 - b_{\mathrm{A}} - b_{\mathrm{E}}} \tag{1}$$

Note that the above linearised system, of the transformed subsystem (21) with $\gamma = \gamma^*$ has a zero eigenvalue which is simple [24], thus the centre manifold theory can be used to analyse the dynamics of (21) near the chosen bifurcation parameter, [33]. To this end, theorem 4.1 of [32] will be used to show the LAS of the endemic equilibrium point of (1) as transformed in (21) for $\gamma = \gamma^*$

Eigenvectors of $\mathcal{J}(\mathcal{E}_{\mathrm{R}}^*)$at $\gamma = \gamma^*$

Let $\mathrm{W} = (\mathrm{w}_1, \mathrm{w}_2, \mathrm{w}_3, \mathrm{w}_4, \mathrm{w}_5)^t$and $\mathrm{V} = (\mathrm{v}_1, \mathrm{v}_2, \mathrm{v}_3, \mathrm{v}_4)$be the corresponding right and left eigenvectors associated with the zero eigenvalues of the Jacobian $\mathcal{J}_{\gamma^*}$. Then for:

$$\mathrm{V}\mathcal{J}(\mathcal{E}_{\mathrm{R}}^0) = \begin{pmatrix} \mathrm{v}_1 \\ \mathrm{v}_2 \\ \mathrm{v}_3 \\ \mathrm{v}_4 \\ \mathrm{v}_5 \end{pmatrix} \begin{pmatrix} -\eta_{\mathrm{N}} & 0 & 0 & -(\beta_{\mathrm{A}} + \beta_{\mathrm{E}}) & -\phi_{\mathrm{P}}\beta_{\mathrm{E}} \\ 0 & -\eta_{\mathrm{B}} & \lambda_{\mathrm{R}} & 0 & 0 \\ 0 & 0 & -\eta_{\mathrm{R}} & 0 & 0 \\ \eta_{\mathrm{N}} & \eta_{\mathrm{B}} & \eta_{\mathrm{R}} & \beta_{\mathrm{A}} + \beta_{\mathrm{E}} - K_1 & \phi_{\mathrm{P}}\beta_{\mathrm{E}} \\ 0 & 0 & \eta_{\mathrm{R}} & \lambda + \xi & -\gamma \end{pmatrix} = \begin{pmatrix} 0 \\ 0 \\ 0 \\ 0 \\ 0 \end{pmatrix}$$

Thus the left eigenvalues are

$$\mathrm{v}_1 = \mathrm{v}_2 = \mathrm{v}_4, \mathrm{v}_3 = \frac{\lambda_{\mathrm{R}}\mathrm{v}_1 + \eta_{\mathrm{R}}(\mathrm{v}_4 + \mathrm{v}_5)}{\eta_{\mathrm{R}}}, \mathrm{v}_1 = \frac{(\beta_{\mathrm{A}} + \beta_{\mathrm{E}} - K_1)\mathrm{v}_4 + (\lambda + \xi)\mathrm{v}_5}{\beta_{\mathrm{A}} + \beta_{\mathrm{E}}},$$

$$\mathrm{v}_5 = \frac{\phi_{\mathrm{P}}\beta_{\mathrm{E}}(\mathrm{v}_4 - \mathrm{v}_1)}{\gamma} = 0 \Longrightarrow \mathrm{v}_1 = \frac{\beta_{\mathrm{A}} + \beta_{\mathrm{E}} - K_1}{\beta_{\mathrm{A}} + \beta_{\mathrm{E}}}\mathrm{v}_4, \text{and } \mathrm{v}_3 = \frac{\lambda_{\mathrm{R}}\mathrm{v}_1 + \eta_{\mathrm{R}}\mathrm{v}_4}{\eta_{\mathrm{R}}}$$

Similarly, the right eigenvector as computed thus

$$\mathcal{J}(\mathcal{E}_{\mathrm{R}}^0)\mathrm{W} = \begin{pmatrix} -\eta_{\mathrm{N}} & 0 & 0 & -(\beta_{\mathrm{A}} + \beta_{\mathrm{E}}) & -\phi_{\mathrm{P}}\beta_{\mathrm{E}} \\ 0 & -\eta_{\mathrm{B}} & \lambda_{\mathrm{R}} & 0 & 0 \\ 0 & 0 & -\eta_{\mathrm{R}} & 0 & 0 \\ \eta_{\mathrm{N}} & \eta_{\mathrm{B}} & \eta_{\mathrm{R}} & \beta_{\mathrm{A}} + \beta_{\mathrm{E}} - K_1 & \phi_{\mathrm{P}}\beta_{\mathrm{E}} \\ 0 & 0 & \eta_{\mathrm{R}} & \lambda + \xi & -\gamma \end{pmatrix} \begin{pmatrix} \mathrm{w}_1 \\ \mathrm{w}_2 \\ \mathrm{w}_3 \\ \mathrm{w}_4 \\ \mathrm{w}_5 \end{pmatrix} = \begin{pmatrix} 0 \\ 0 \\ 0 \\ 0 \\ 0 \end{pmatrix}$$

has the following associated values

$$\mathrm{w}_1 = -\frac{(\beta_{\mathrm{A}} + \beta_{\mathrm{E}})\mathrm{w}_4 + \phi_{\mathrm{P}}\beta_{\mathrm{E}}\mathrm{w}_5}{\eta_{\mathrm{N}}}, \mathrm{w}_2 = \mathrm{w}_3 = 0, \mathrm{w}_4 = \frac{\eta_{\mathrm{N}}\mathrm{w}_1 + \phi_{\mathrm{P}}\beta_{\mathrm{E}}\mathrm{w}_5}{K_1 - (\beta_{\mathrm{A}} + \beta_{\mathrm{E}})}, \mathrm{w}_5 = \frac{\lambda + \xi}{\gamma}\mathrm{w}_4$$

itthus follows from (6)that if$\mathrm{v}_4 > 0$, then $\mathrm{v}_1 = \mathrm{v}_2 > 0 \Longrightarrow \mathrm{v}_3 > 0;\ \mathrm{v}_5 > 0$.Also if $\mathrm{w}_4 > 0$, then $\mathrm{w}_1 > 0$ and $\mathrm{w}_5 > 0$.

Computations of a **and** b**:**

Noting that at RFE$\eta_{\mathrm{p}}^* = 0$, then the derivatives of the transformed system (21) are computed thus:

$$\frac{\partial^2 f_1}{\partial x_1^2}=\frac{\partial^2 f_1}{\partial x_1\partial x_2}=\frac{\partial^2 f_1}{\partial x_1\partial x_3}=0,\frac{\partial^2 f_1}{\partial x_1\partial x_4}=\frac{\partial^2 f_1}{\partial x_4\partial x_1}-1,\frac{\partial^2 f_1}{\partial x_1\partial x_5}=\frac{\partial^2 f_1}{\partial x_5\partial x_1}=-\frac{\eta_{\mathrm{N}}\phi_{\mathrm{P}}\beta_{\mathrm{E}}}{\Pi}$$
$$\frac{\partial^2 f_4}{\partial x_1\partial x_4}=\frac{K_1(\beta_{\mathrm{A}}+\beta_{\mathrm{E}})}{\Delta+\Pi},\frac{\partial^2 f_4}{\partial x_1\partial x_5}=\frac{\phi_{\mathrm{P}}\beta_{\mathrm{E}}K_1}{\Delta+\Pi},\frac{\partial^2 f_5}{\partial x_3\partial x_5}=\frac{\partial^2 f_5}{\partial x_5\partial x_3}=\eta_{\mathrm{R}}$$

Then

$$\boldsymbol{a}=\frac{\mathbf{v_1w_1}}{\mathbf{2}}\left\{\frac{\boldsymbol{K_1}}{\boldsymbol{\Delta+\Pi}}[(\boldsymbol{\beta_{\mathrm{A}}}+\boldsymbol{\beta_{\mathrm{E}}})\mathbf{w_4}+\boldsymbol{\phi_{\mathrm{P}}\beta_{\mathrm{E}}}\mathbf{w_5}]-\mathbf{2}\frac{\mathbf{w_4\Pi}+\boldsymbol{\eta_{\mathrm{N}}\phi_{\mathrm{P}}\beta_{\mathrm{E}}}\mathbf{w_5}}{\boldsymbol{\Pi}}\right\}$$

from which it can be verified that

$$\boldsymbol{a}=\frac{\mathrm{v_1w_1w_4}}{\mathbf{2}\boldsymbol{\gamma}}\left\{\frac{K_1[\boldsymbol{\gamma}(\beta_{\mathrm{A}}+\beta_{\mathrm{E}})+\phi_{\mathrm{P}}\beta_{\mathrm{E}}(\boldsymbol{\lambda}+\boldsymbol{\xi})]}{\Delta+\Pi}-\frac{\mathbf{2}[\boldsymbol{\gamma\Pi}+\eta_{\mathrm{N}}\phi_{\mathrm{P}}\beta_{\mathrm{E}}(\boldsymbol{\lambda}+\boldsymbol{\xi})]}{\Pi}\right\}=-\mathbf{1.7426}\mathrm{v_1w_1w_4}<0$$

Similarly, computing for b, with the following derivatives,

$$\frac{\partial^2 f_4}{\partial x_4\partial\gamma^*}=-1,\frac{\partial^2 f_4}{\partial x_5\partial\gamma^*}=-1.$$

We have

$$\mathbf{b}=-\mathbf{v_4w_4}<0$$

Thus, $a<0, b<0$.. Therefore following Theorem 6, item (ii), we have established the following result (note that this result holds for $\mathcal{D}_{\mathrm{R}}>1$but close to 1):

Theorem 8: The unique persistence equilibrium guaranteed by Theorem 7 is LAS for $\mathcal{D}_{\mathrm{R}}$ near 1.

In summary, the model (1) has a globally-asymptotically stable RFE whenever $\mathcal{D}_{\mathrm{R}}<1$, and a unique persistence equilibrium point whenever $\mathcal{D}_{\mathrm{R}}>1$. Theunique persistence equilibrium point is LAS at least near $\mathcal{D}_{\mathrm{R}}=1$.

3.0 Numerical Simulation

Table 2. Description of model parameters

Parameter	Description	Baseline value	Reference
D	Natural fertility growth rate of fertile	0.43	Implied from [34]
Ω	Constant manure generation rate	0.3	[35]
F	Animal population	1.3	[34]
Π	Aggregate external pressure rate	10	[36]
g	Soil loss to development	1.77	[34]
l	Soil loss to infertility	2.8	[34]
y	Livestock removal rate	0.1	Assumed
x	Soil loss to erosion	0.75	Assumed
f_{P}	Modification parameter	0.6	Implied from [34]
h_{R}	Livestock/soil interaction rate	0.01	Assumed
h_{B}	Manure decomposition rate	0.75	Assumed
h_{N}	Soil depletion advocacy rate factor	0.95	Assumed
l_{R}	Harvested livestock droppings rate	0.35	Assumed
b_{A}	Anthropological effective contact rate(AECR)	0.043	[37]
b_{E}	Erosion effective contact rate(EECR)	0.263	[37]

In this section, we perform computer simulations to present graphic representations of the results obtained in the immediate section. Pursuant to this, we will use the data presented in table 2, so that the corresponding component values of our positive equilibrium, $\mathrm{E}_{\mathrm{R}}^*$, becomes

$$\boldsymbol{\mathcal{P}^*=8.64412,\mathcal{B}^*=6.46667,\mathcal{R}^*=13.00000,\mathcal{S}_{\mathrm{V}}^*=1.10487,\mathcal{S}_{\mathrm{Nv}}^*=2.53799}(2)$$

It is found by (23) that condition (4) is satisfied since, as can be verified $\mathcal{D}_{\mathrm{R}}=0.11700<1$thus by lemma 1 and lemma 2 the RFE of (1) is, both, LAS and GAS, respectively. It can also be verified that by (23) and lemma 5 the RFE has no instance of a continuous non-rearing equilibrium.

To further monitor the effects of the baseline parameters on both topsoil fertility growth and depletion, we herewith present various computer simulations using MATLAB.

Figures 1, 2 and 3predict the enormous potential of increasing manure decomposition, increased manure harvest and livestock/soil interaction, respectively to support higher vegetation growth on both soil types. This could be due to the expected respective increases in manure deposition and absorption. However, we note that while manure absorption appears to lack the capacity to sustain the gains, probably due to uncontrollable high grazedensity; those of livestock/soil interaction and manure harvest suggest an increasing growth path. We further note the very sharp impact rate of the former as compared to the gradual cases of both interaction and harvest. It can also be observed that when the former began its fall, the other two cases showed an increasing impact.

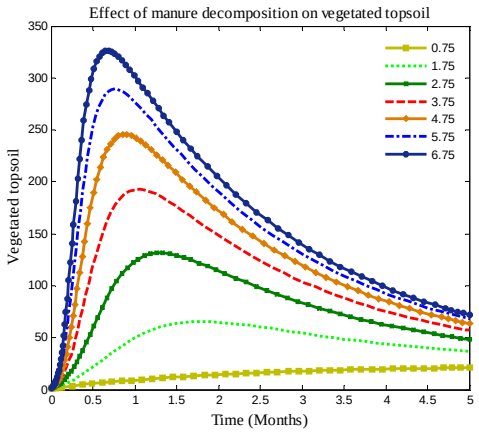

Figure 1a. Plot of vegetated topsoil, S_V, against time for different values of h_B as obtained from Table 2

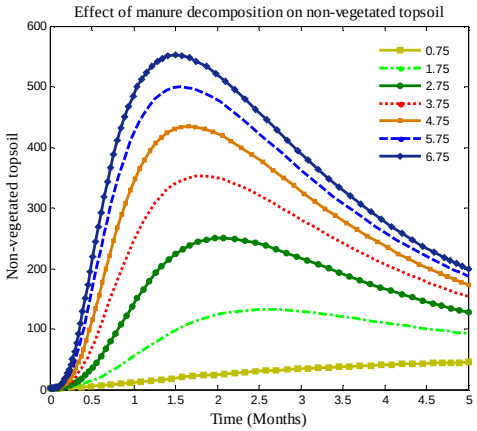

Figure 1b: Plot of non-vegetated topsoil, S_{Nv}, against time for different values of h_B as obtained from Table 2

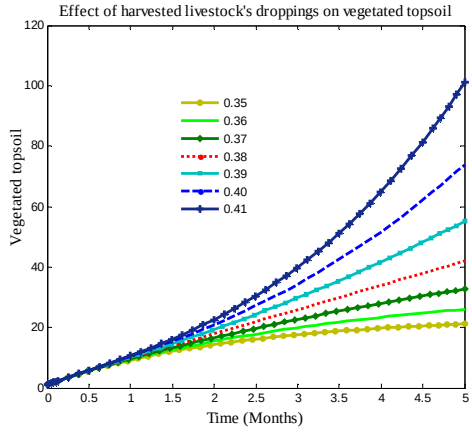

Figure 2a: Plot of vegetated topsoil, S_V, against time for different values of l_R as obtained from Table 2

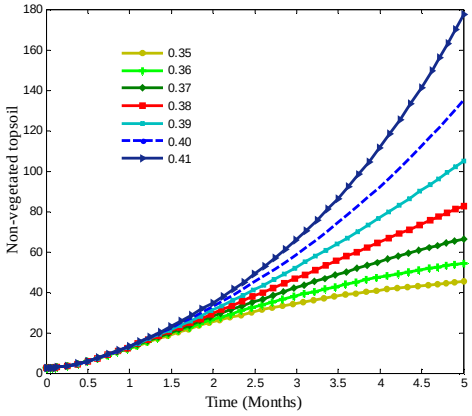

Figure 2b: Plot of non-vegetated topsoil, S_{Nv}, against time for different values of l_R as obtained from Table 2

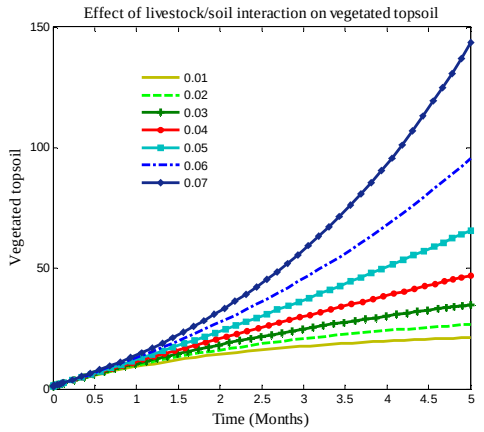

Figure 3a: Plot of vegetated topsoil, S_V, against time for different values of h_R as obtained from Table 2

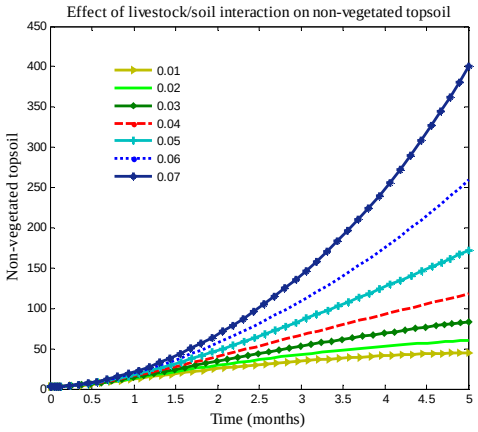

Figure 3b: Plot of non-vegetated topsoil, S_{Nv}, against time for different values of h_R as obtained from Table 2

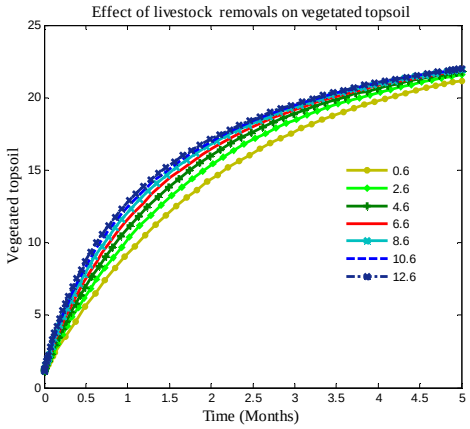

Figure 4a: Plot of vegetated topsoil, S_V, against time for different values of y as obtained from Table 2

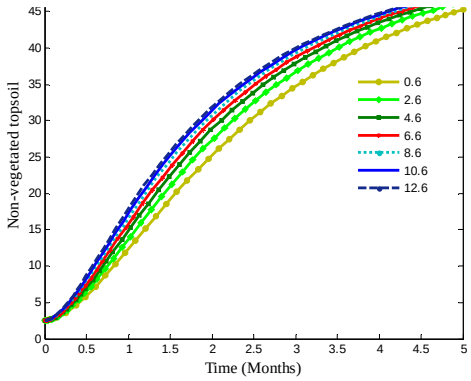

Figure 4b: Plot of non-vegetated topsoil, S_{Nv}, against time for different values of y as obtained from Table 2

Figure 4 on its pact suggests that reducing livestock density (either through consumption or death) can increase, though marginally, vegetation growth. In figures 5, 6, 7 and 8 we note that each of human induced vegetation removal (HIVR), natural-induced vegetation removal (NIVR), none agricultural land utilisation (NALU) and environmental enlightenment/advocacy campaigns has the capacity to reduce vegetation growth, the NALU having a substantial impact on non-vegetated topsoil.

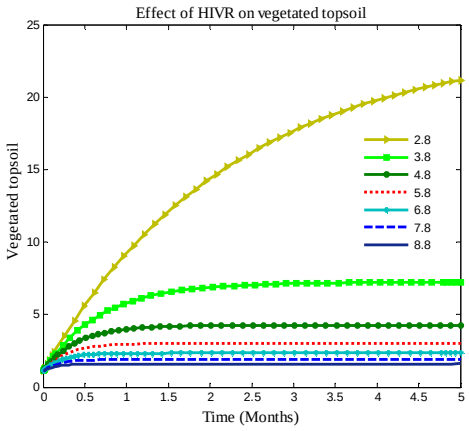

Figure 5a: Plot of vegetated topsoil, S_V, against time for different values of l as obtained from Table 2

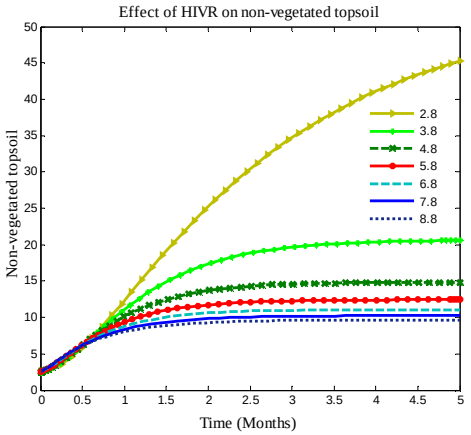

Figure 5b: Plot of non-vegetated topsoil, S_{Nv}, against time for different values of l as obtained from Table 2

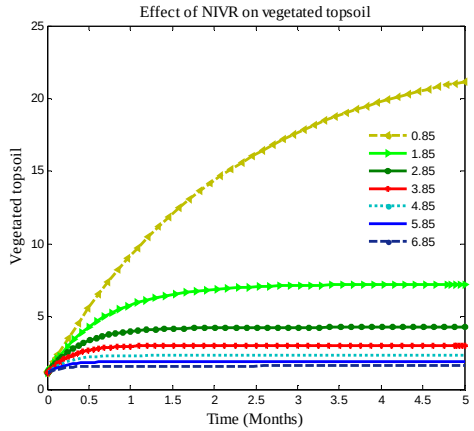

Figure 6a: Plot of vegetated topsoil, S_V, against time for different values of x as obtained from Table 2

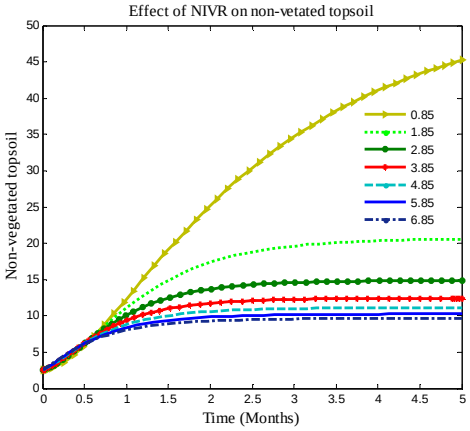

Figure 6b: Plot of non-vegetated topsoil, S_{Nv}, against time for different values of x as obtained from Table 2

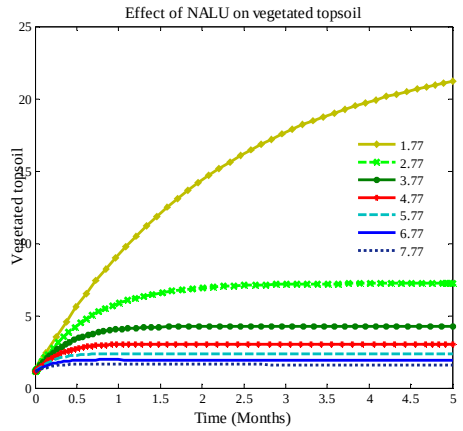

Figure 7a: Plot of vegetated topsoil, S_V, against time for different values of x as obtained from Table 2

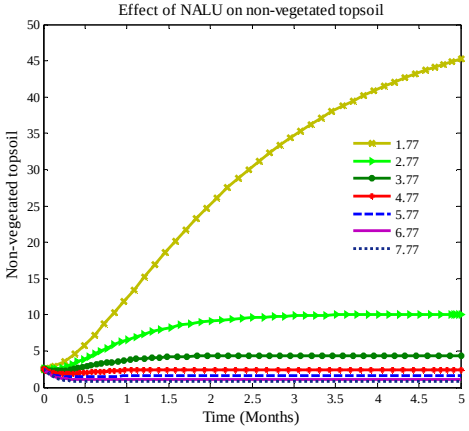

Figure 7b: Plot of non-vegetated topsoil, S_{Nv}, against time for different values of x as obtained from Table 2

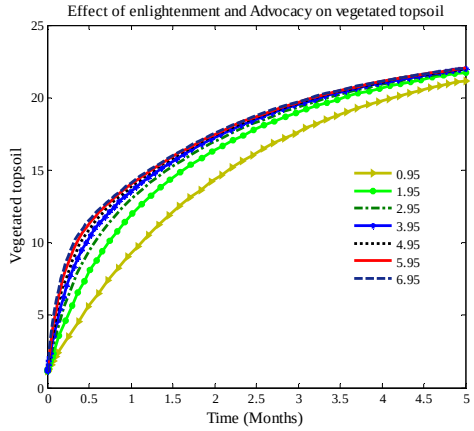

Figure 8a: Plot of vegetated topsoil, S_V, against time for different values of h_N as obtained from Table 2

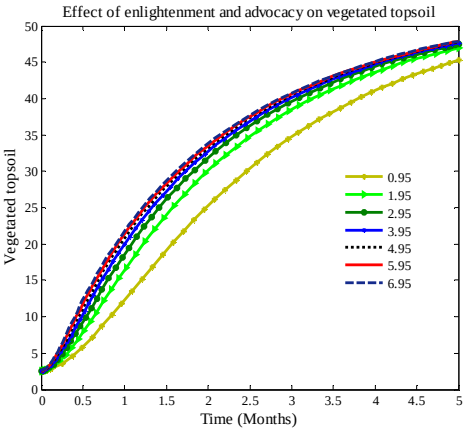

Figure 8b: Plot of non-vegetated topsoil, S_{Nv}, against time for different values of h_N as obtained from Table 2

5.0 Conclusion

In this paper, we presented a system of mathematical model equations to study the impact of organic rearing on fertile topsoil.Extension and other forms of advocacy and enlightenments we found to have positive impact on sustain the environment. To further support this fact, we also showed that when the efforts are excessively deployed on the soil (overgrazing) beyond the sustainable threshold, vegetation coverbegin to deplete. The reallocation of soils to NALUis shown to also contribute to vegetation loss. The GAS status of our model implies its global applicability. It has become evidently clear that the first month of the grazing schedule is the most critical. We advocate the simultaneous combination of manure harvest (which could also control wastages), sustainable grazing and sustainable manure disposal (to control excessive ethane and other greenhouse gas emissions).

4.0 Reference

[1] FAO (2002). “Good Agricultural practices”. Second version. FAO, Rome.

[2] Rota, A and Sperandini, S. (2010). Integrated crop-livestock systems. IFAD, Rome

[3] von Grebmer, K., Headey, D., Béné, C., Haddad, L., Olofinbiyi, T., Wiesmann, D., Fritschel, H., Yin, S., Yohannes, Y., Foley, C., von Oppeln, C. and Iseli, B. (2013). *2013 Global Hunger Index: The Challenge of Hunger: Building Resilience to Achieve Food and Nutrition Security*. Bonn, Washington, DC, and Dublin: Welthungerhilfe, International Food Policy Research Institute, and Concern Worldwide

[4] Wu, S-H., Ho, C-T., Nah, S-L and Chau, C-F. (2014) Global Hunger: A Challenge to Agricultural, Food, and Nutritional Sciences, Critical Reviews in Food Science and Nutrition, 54:2, 151-162, DOI: 10.1080/10408398.2011.578764

[5] Pearson, R.A., (1993). Strategic research on nutrition and management of draught animals. In: Proceedingsof a Workshop on Human and Draught Animal Power in Crop Production, 18–22 January 1993,Harare, Zimbabwe.

[6] Rosenzweig C. & Parry L. (1994). "Potential impact of climate change on world food supply," Nature, Vol. 367, pp. 133- 138

[7] Karing, P, Ain, K. and Heino, T. (1999). "Adaptation principles of agriculture to climate change," Climate Research, Vol. 12, No. 2-3, pp. 175-183

[8] Intergovernmental Panel on Climate Change (IPCC). 2001. “Climate Change 2001: Impacts, Adaptation and Vulnerability”. (Chapter 10) Cambridge University Press

[9] Zhou, Y. (2010). Smallholder Agriculture, Sustainability and the Syngenta Foundation. Syngenta Foundation for Sustainable Agriculture April 2010

[10] Mailumo, S., Ben, A and Omolehin, R. (2013). Analysis of Poverty-Environmental Degradation Nexus among Arable Crop Farmers in Plateau State, Nigeria. Journal of Economics and Sustainable Development. www.iiste.org ISSN 2222-1700 (Paper) ISSN 2222-2855 (Online) Vol.4, No.8, 2013

[11] McKyes, E., 1984. Prediction and field measurements of tillage tool draft forces and efficiency in cohesivesoils. Soil and Tillage Research 4, 459–470

[12] Betker, J., Kutzbach, H.D., 1989. Influence of design on the draught force characteristics of animal-drawncarts. In: Draught Animals in Rural Development. ACIAR Proceedings Number 27, pp. 258–263)

[13] Starkey, P., 1989. Harnessing and Implements for Animal Traction: an Animal Traction Resource Bookfor Africa. GATE, ESchborn, Germany.

[14] Inns, F.M., 1990. The mechanics of animal-draught cultivation implements. Agricultural Engineer 45 (1),13–16

[15] Mupeta, B., Ndlovu, L.R., Prasad, V.L., 1990. The effect of work and level of feeding on voluntary foodintake, digestion, rate of passage and body weight in Mashona oxen given low quality roughage. Zimbabwe Journal of Agricultural Research 28, 18–21

[16] Pearson, R.A., Smith, A.J., 1992. Improving draught animal management. In: Starkey, P., Mwenga, E.,Stares, J. (Eds.), Improving animal traction technology. Proceedings of the animal traction network forEastern and Southern Africa (ATNESA), 18–23 January. Lusaka, Zambia, pp. 122–129

[17] Matthewman, R.W., Dijkman, J.T., 1993. The nutrition of draught animals. Journal of AgriculturalScience, Cambridge 121, 297–306

[18] Bartholomew, P.W., Khibe, T., Little, D.A., Ba, S., 1994. Effect of change in body weight and conditionduring the dry season on capacity for work of draft oxen. Tropical Animal Health and Production 25,50–58.

[19] Cros, M. J., Duru, M., Garcia, F.& Martin-Clouaire, R. (2004). Simulating Management Strategies: The Rotational Grazing Example. Agric. Syst. 80, 23–42

[20] Dixon, J. & Gulliver, A. (2001). "Farming Systems and Poverty Improving Farmers' Livelihoods in a Changing World" FAO, Rome and World Bank, Washington D.C.

[21] FGN, (2009). "Report of the Vision 2020 National Technical Working Group on Agriculture & Food Security"

[22] Chawatama, S., Ndlovu, L.R., F.D. Richardson, F.D., Mhlanga, F and Dzama, K (2000). A simulation model of draught animal power insmallholder farming systems. Part I: Context and structural overview. Agricultural Systems 76 (2003) 415–440

[23] Vélez, M., Hernández, D., Bernier, U., van Laarhoven, J. and Camacho, E. (2003). Mathematical Models for Photoreceptor Interactions. Mathematical and Theoretical Biology Institute, USA. Pp 25 – 67

[24] Sharomi, O., Podder, C., Gumel, A. and Song, B. (2008). Mathematical Analysis of the Transmission Dynamics Of HIV/TB Coinfection in the Presence of Treatment Mathematical Biosciences and Engineering Vol. 5, Number 1, January 2008 pp. 145–174

[25] Hethcote, W.H. (2000). The Mathematics of Infectious Diseases. SIAM Review. 42(4): 599-653.

[26] Wang, X and Ma, H. (2012). A Lyapunov Function and Global Stability for a Class of Predator-Prey Models. Discrete mathematics in Nature and Society.

[27] Driessche, P. van den and J. Watmough, J. (2002). Reproduction Numbers and Sub-Threshold Endemic Equilibria for Compartmental Models of Disease Transmission. Mathematical Biosciences. 180: 29-48.

[28] Ameh, J. E. (2009). The Basic Reproductive Number: Bifurcation and Stability. African Institute for Mathematical Sciences (AIMS, postgraduate diploma at AIMS.

[29] Diekmann, O., Heesterbeek, J.A.P. & Metz J.A.J. (1990). On the Definition and the Computation of the Basic Reproduction Ratio R_0 in Models for Infectious Diseases in Heterogeneous Populations, J. Math. Biol. 28 (1990) 365.

[30] Castillo-Chevez, C., Feng, Z and Huang, W. On the Computation of R_0 and its Role on Global Stability, in Castillo-Chavez, C., Blower, S., Van den Driessche, P., Krirscner, D. and Yakubu, A. (2002). Mathematical Approaches for Emerging and Re-emerging Infectious Diseases: An introduction. The IMA Volumes in Mathematics and its Applications. Springer Verlag, New York 125229-250.

[31] Sirajo, A. (2014). A Mathematical Model for the Transmission Dynamics and Control of Hepatitis B Virus. *PhD Thesis*, FUT, Minna

[32] Castillo-Chavez, C. & Song, B. (2004). Dynamical Model of Tuberculosis and their Applications. Mathematical Biosciences and Engineering. 1:361-404.

[33] Carr, J. (1981). Applications of Centre Manifold Theory. Springer-Verlag, New York

[34] Birte, J., Abaidoo, R., Chikoye, D. &Stahr, K. (2008).soil Conservation in Nigeria: Past and Present On-station and On-farm Initiatives. Soil and Water Conservstion Society, USA. 800-THE-SOIL (800-843-7645). www.swcs.org

[35] Okwuagwu, M.I., Alleh, M.E. and Osemwota, I. O. (2003). The Effects of Organic and Inorganic Manure on Soil Properties and Yield of Okra in Nigeria. African Crop Science Conference Proceedings, Vol. 6. 390-393. Printed in Uganda. All rights reserved. ISSN 1023-070X $ 4.00 © 2003, African Crop Science Society

[36] Dubey, B. (2005). A Nonlinear Model for Topsoil Erosion Caused by Heavy Rain. *Nonlinear Analysis: Modelling and Control*. Vol. 10, No. 1, 35–56

[37] Ogwuche, J. &Bulus, J. (2013). Geospatial Application in Mapping Gully Erosion Sites in Jos, Plateau State, Nigeria. Scholarly Journal of Scientific Research and Essay (SJSRE) Vol. 2(6), pp. 85 – 95, June 2013